

First Principles Calculations of Fe on GaAs (100).

S. Mirbt, B. Sanyal, C. Isheden, and B. Johansson
Department of Physics, Uppsala University, Uppsala, Sweden
(Dated: October 31, 2018)

We have calculated from first principles the electronic structure of 0.5 monolayer upto 5 monolayer thick Fe layers on top of a GaAs (100) surface. We find the Fe magnetic moment to be determined by the Fe-As distance. As segregates to the top of the Fe film, whereas Ga most likely is found within the Fe film. Moreover, we find an asymmetric in-plane contraction of our unit-cell along with an expansion perpendicular to the surface. We predict the number of Fe 3d-holes to increase with increasing Fe thickness on *p*-doped GaAs.

PACS numbers: 75.70.-i, 82.65.+r, 75.50.Bb, 72.25.Mk

I. INTRODUCTION

In the context of magnetoelectronics it is important to understand the structural and electronic properties of the interface between Fe and GaAs [1, 2]. Several experimental investigations have been performed on this interface [3, 4, 5, 6, 7, 8, 9, 10, 11, 12, 13, 14, 15, 16, 17]. Under As-rich conditions the Fe film growing on top of GaAs is found to have a reduced magnetic moment, or even a zero magnetic moment close to the interface [3, 4, 5]. Moreover, structural investigations of the Fe film lead to the conclusion that between a bcc Fe film and the GaAs substrate there exists an intermediate phase, $Fe_xGa_yAs_z$ [6, 7]. Under Ga-rich conditions no traces of an intermediate phase are found and the magnetic moment is found to be bulk-like even close to the interface [8, 9].

Other theoretical investigations of the Fe/GaAs(100) interface [18, 19, 20, 21] have been performed. Except of the calculations by Erwin et al [20], all other calculations considered only an ideal Fe/GaAs interface. Erwin focused on Fe adatom growth and magnetic properties of the interface and allowed for ionic relaxations only perpendicular to the surface (i.e along the *z*-direction). In general their results agree with our calculations. In this paper we present an investigation of the (completely) relaxed Fe/GaAs interface structure. We study the Fe magnetic moment as a function of the Fe film thickness and the relaxed structure of the Fe film. In addition we study As and Ga segregation. We discuss the origin of the so called magnetically dead layers on top of GaAs and why Fe growth differs on As terminated and Ga terminated interfaces.

II. COMPUTATIONAL DETAILS

We have performed self-consistent first-principles density functional calculations employing a plane wave pseudopotential code (VASP) [22]. PAW pseudopotentials [23] with an energy cutoff of 24.61 Ryd were used. Exchange correlation was treated within the generalized gradient approximation (GGA) [24]. We used a (4x4x4) folding of special *k*-points [25]. We used a unit cell having 6 semiconducting layers (3 Ga and 3 As) as the sub-

strate and 1 to 10 Fe atoms (0.5 monolayer to 5 monolayers) on top of the GaAs substrate. A vacuum of 10 Å thickness or more was kept to avoid interactions between neighboring unit cells in the (001) direction. To simulate a bulk semiconductor, the lowermost Ga/As layer was passivated with pseudohydrogen atoms [26]. Volume and shape relaxations were allowed along with the relaxation of the atoms. All atoms were relaxed except the 2 bulk semiconducting atoms. It is worth mentioning that the bcc Fe is perfectly lattice matched to the GaAs substrate (zinc-blende lattice). The GaAs lattice constant (5.65 Å) is almost twice of the lattice constant of bcc Fe (2.87 Å). Thus the GaAs unit cell is equivalent to two bcc unit cells. We used a lattice constant of 5.735 Å which corresponds to the calculated GaAs bulk equilibrium lattice constant within GGA. The lattice constant of bulk Fe is calculated to be only 0.05% smaller. The energies were converged with an accuracy of 10^{-4} eV. The Pulay stress we find to be negligible, being of the order of 0.1 kBar.

Local magnetic moments were obtained by projecting wave functions onto spherical harmonics within spheres centered on the atoms [27]. We used 1.302 Å, 1.402 Å and 1.355 Å for Fe, Ga, and As spheres, respectively. In order to compare energies of different interface geometries with a non-equivalent number of atoms, we used the following definition of the formation energy:

$$E_{form} = E_{total} - \sum_i N_i \mu_i. \quad (1)$$

N_i is the number of non equivalent atoms of species *i*, and μ_i is the chemical potential. We estimated the chemical potential by calculating the total energy of species *i* in its bulk form.

III. GAAS SURFACE

The GaAs (100) surface structure depends on the growth environment. Under As rich conditions the GaAs (100) surface shows a c(4x4) [28] reconstruction, whereas under Ga rich conditions the GaAs (100) surface shows an ϵ (4x2) [29] reconstruction. All these reconstructions differ from an ideally terminated surface -where either

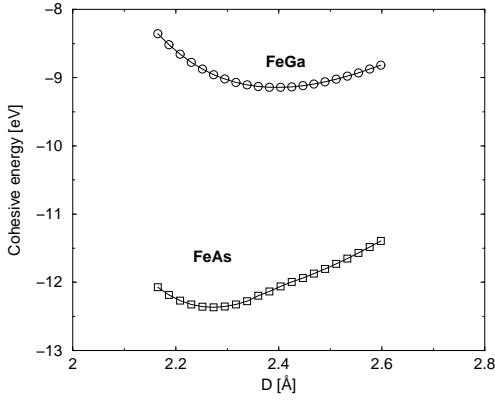


FIG. 1: Cohesive energy as a function of the Fe-X distance ($X=\text{As}, \text{Ga}$) for a bulk zincblende FeX structure. The upper curve (circles) corresponds to zincblende FeGa, the lower curve (squares) to zincblende FeAs.

only Ga or only As exists at the surface- by the existence of Ga-Ga and (or) As-As dimers.

In a first attempt to understand the interface between Fe and GaAs we neglect any surface reconstructions and assume an ideal Ga(As) terminated surface. In order to justify this approximation, let us assume we would grow Fe on top of some reconstructed GaAs surface. The interaction of Fe with the dangling bonds of As or Ga is already included in our calculation assuming an ideal cut. The question is now what happens with the As-As (Ga-Ga) dimers, when Fe is present at the surface? In a recent paper Erwin et al. [20] calculate that Ga and As surface dimers become unstable under Fe adsorption and Fe-Ga resp. Fe-As bonds form instead. This implies that our calculation assuming an ideal cut surface covers most of the physics at the Fe-GaAs interface. Moreover, experimental results by Kneeder et al. [16] warrant our approximation to ignore the surface reconstruction details. They investigated the influence of the GaAs surface reconstructions on the properties of the growing Fe film. They compared two As-rich terminations, the 2×4 and the $c(4\times 4)$. In summary they find, although the Fe island morphology is different, the growth mode, interfacial structure, magnetic behaviour, and the uniaxial anisotropy to be independent on the chosen As-rich surface reconstruction.

The difference in Fe growth between a Ga-terminated and an As-terminated surface can be explained largely by kinetic arguments. In Fig.1 we show the cohesive energy as a function of the Fe-Ga (Fe-As) distance for bulk FeGa (FeAs) in a zincblende structure. (These artificial structures only serve as a tool to understand the FeAs and FeGa interaction.) The cohesive energy of zincblende FeAs is about 4 eV lower than of FeGa. Thus the interaction between Ga and Fe is much weaker than between As and Fe, because As has three p -electrons and Ga only one p -electron, which gives rise to a larger pd -hybridization between As and Fe. According to Eq.2, energy is gained, when Fe replaces a Ga atom. There-

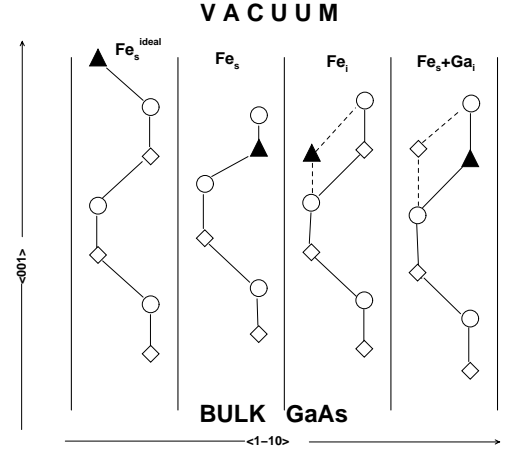


FIG. 2: Geometrical structure of 0.5 ML Fe on top of GaAs(100). Circles (diamonds) represent As (Ga) and triangles represent Fe. The four columns correspond to four different interface configurations as discussed in the text. The atomic positions are shown along the $\langle 1\bar{1}0 \rangle$ direction, bonds are indicated by the lines connecting the atoms.

fore, if it is kinetically possible, Fe replaces a Ga atom in the interface region independent of the surface termination. In addition, energy is gained, -independently of the termination-, if As segregates to the surface (see section VI). The experimentally observable physical properties of the Fe on GaAs(100) system are thus governed by extrinsic effects like growth conditions and in addition the surface termination governs the kinetic conditions for the Fe growth, i.e the height of involved barriers, diffusion probability, probability distribution of As atoms versus Ga atoms within the Fe film.

In this paper we discuss the physical properties of an Fe film on an As-terminated surface, but our conclusions are valid independent of the termination, since we do not calculate any kinetic properties.

IV. STRUCTURAL PROPERTIES

In GaAs bulk an Fe impurity is most likely found in a Ga-substitutional position, i.e Fe replaces a Ga atom. For 0.5 ML Fe on top of a (100) GaAs surface, we compare here four different Fe configurations (Fig.2). We show the four different Fe configurations in the order of decreasing formation energy: Fe_s^{ideal} corresponds to one Fe atom (i.e. 0.5 ML) sitting on top of GaAs at the position of a Ga atom, that is Fe sits substitutionally (s) following the ideal stacking (no lattice relaxations). Fe_s corresponds to one Fe atom having replaced the Ga atom closest to the surface, that is the Fe atom becomes buried under the surface. Fe_i corresponds to one Fe atom sitting in a buried position but at an interstitial (i) position of the ideal GaAs lattice. $Fe_s + Ga_i$ finally corresponds to one Fe atom sitting in a substitutionally buried position, but in addition a Ga atom is now sitting in an interstitial

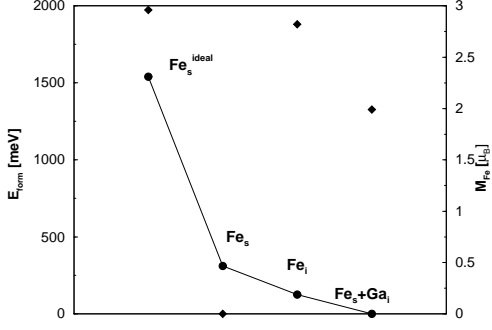


FIG. 3: Formation energy, E_{form} , of 0.5ML Fe configurations (see Fig.2) relative to the lowest configuration, $Fe_s + Ga_i$. Also indicated is the magnetic moment of the Fe atom (right scale and diamonds).

position.

In Fig.3 we show the formation energy relative to the formation energy of the $Fe_s + Ga_i$ configuration. Let us now discuss these results: The four configurations differ by the number of vacant neighbours that each Fe atom has: In the Fe_s^{ideal} configuration, Fe has four vacant neighbours, in the Fe_s , Fe has three vacant neighbours, and in the other two configurations, Fe has only two vacant neighbours. The more neighbours the Fe atom has, the more energy is gained due to increased wavefunction overlap. Thus the Fe_s^{ideal} configuration is highest in energy, because the wavefunction overlap between Fe and its surrounding is minimal. Next we consider the Fe_s configuration, which is already 1 eV lower than Fe_s^{ideal} . Besides having one more neighbour than Fe_s^{ideal} , in the Fe_s configuration two Fe-As bonds have formed. For this configuration the Fe magnetic moment is totally quenched. This will be further discussed in the next section. The Fe_i and $Fe_s + Ga_i$ configurations are lower than Fe_s because they only have two vacant neighbours. These two configurations are similar except that the topmost Ga and Fe positions have been interchanged. We find from our calculation

$$E_{Ga-As} + E_{Fe_i} > E_{Fe-As} + E_{Ga_i}, \quad (2)$$

where E_{Ga-As} (E_{Fe-As}) is the formation energy of a Ga-As (Fe-As) surface bond and E_{Fe_i} (E_{Ga_i}) is the formation energy of an interstitial surface defect Fe_i (Ga_i).

We compared the charge density and performed an (unrelaxed) calculation without the respective interstitial atom. In both configurations, the top Ga atom forms together with the Fe atom a metallic layer. The difference is the bonding: For Fe_i we have mainly two Ga-As bonds and one Ga-Fe metallic bond, whereas for $Fe_s + Ga_i$ we have two Fe-As bonds and again one Ga-Fe metallic bond, but in addition the interstitial Ga atom bonds to its As neighbours. This Ga_i -As interaction reduces the Fe-As interaction, whereby the Fe magnetic moment is close to its bulk value. It is thus the Ga_i that lowers the energy of the $Fe_s + Ga_i$ configuration. In summary, a

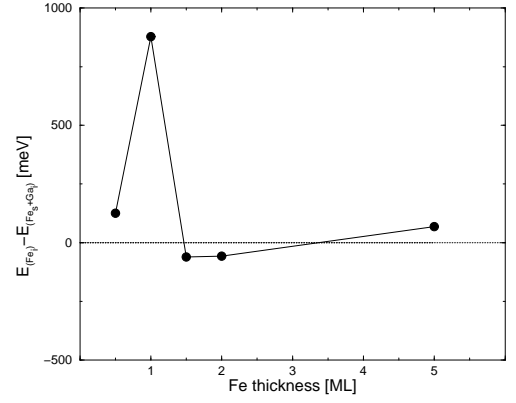


FIG. 4: Energy difference between an interface configuration where Fe sits interstitial (Fe_i) and where Fe sits substitutional together with an interstitial Ga ($Fe_s + Ga_i$) as a function of the Fe film thickness.

TABLE I: Calculated $c/ < a >$ ratio and in-plane lattice contraction of the unit cell along the $< 1\bar{1}0 >$ and $< 110 >$ direction for the lowest energy configuration of the specified Fe film.

	$c/ < a >$	$< 1\bar{1}0 >$	$< 110 >$
0.5 ML Fe	1.07	-1.15 %	-6.92 %
1 ML Fe + 0.5 ML As	1.03	-0.51 %	-3.66 %
1 ML Fe + 1ML As	1.02	+0.86 %	-2.79 %
2 ML Fe + 0.5 ML As	1.10	-0.81 %	-5.61 %
2 ML Fe + 1 ML As	1.05	+0.86 %	-2.79 %
5 ML Fe + 0.5 ML As	1.04	-1.15 %	-2.74 %
5 ML Fe + 1 ML As	1.03	+0.51 %	-1.83 %

dilute (sub-monolayer) Fe film on top of GaAs (100) will break the top GaAs bonds and create Fe-As bonds and Ga_i instead.

Even for thicker Fe films this is in principle still valid. But an Fe interface atom bounded to an Fe film will have a reduced mobility compared to an Fe adatom. This might prevent Fe from dissolving GaAs. This kinetic issue we have not studied any further. We calculate an Fe_s^{ideal} IC to be preferred if As and Ga segregation is neglected. This result is in agreement with a calculation by Erwin et al [20]. But including As surface segregation (still neglecting Ga segregation) we find the $Fe_s + Ga_i$ IC to have the lowest energy almost independent of the Fe film thickness. In Fig.4 we show the energy difference between the Fe_i and $Fe_s + Ga_i$ interface configurations (IC) for a varying number of Fe thickness. For 0.5, 1 and 5 ML of Fe we calculate the $Fe_s + Ga_i$ IC to be lower in energy. On the other hand, for 1.5 and 2 ML of Fe we calculate the Fe_i IC to be lower in energy. It is the exchange energy that stabilizes the Fe_i configuration, since in a non-spin polarized calculation we find again $Fe_s + Ga_i$ to be lower. (This will be further discussed in the next section.) If both As and Ga segregation are included (section VI), we find Fe to dissolve GaAs independent of thickness.

TABLE II: Total magnetic moment and atomic distances for the respective closest topmost atoms for 1ML of Fe for the three interface configurations shown in Fig.6. Ga-As (h) (GaAs (v)) indicates the horizontal (vertical) distance.

	Fe_i	Fe_s+Ga_i start	Fe_s+Ga_i final
Fe - As	2.61 Å	2.42 Å	2.32 Å
Fe - Ga	2.96 Å	2.42 Å	2.51 Å
Ga - As (h)	-	2.87 Å	2.82 Å
Ga - As (v)	-	2.42 Å	3.61 Å
Ga - Ga	-	2.44 Å	2.44 Å
M_{cell}	4.63 μ_B	-	0.01 μ_B

In a recent x-ray absorption fine structure spectroscopy (XAFS) study Gordon et al [11] found the Fe film on GaAs(100) to be tetragonal distorted relative to bulk bcc Fe. The measured distortion involved an in-plane contraction and an expansion perpendicular to the GaAs surface to give a c/a ratio of 1.03. In tab.1 we have collected the calculated c/a ratio as a function of the Fe film thickness and As coverage. Our results agree rather good with experiment. We find in agreement with experiment for our energetically lowest interface configurations an in-plane contraction and an expansion perpendicular to the GaAs surface. In addition we find a rather large asymmetry in the in-plane contraction. In general the contraction along the $\langle 110 \rangle$ direction is larger than along the $\langle 1\bar{1}0 \rangle$ direction. We even find an expansion along the $\langle 1\bar{1}0 \rangle$ direction for all studied Fe coverages which are covered by a complete As monolayer.

The expansion perpendicular to the GaAs surface is connected to the Ga-content within the Fe-film, because for our calculations without any Ga atoms within the Fe-film we find instead a contraction perpendicular to the GaAs surface. The in-plane asymmetry is caused by the directional bonds of the GaAs substrate. On the As-terminated surface, the As dangling bonds are oriented along the $\langle 1\bar{1}0 \rangle$ direction. Because of the Fe-As interaction and the $Fe_s + Ga_i$ IC, an expansion/contraction along the $\langle 11\bar{0} \rangle$ direction has to optimize the Fe-As interaction. In contrast, an expansion/contraction along the $\langle 110 \rangle$ direction is a reaction on the expansion/contraction along the other two directions in order to optimize the overall volume. Therefore, the $\langle 11\bar{0} \rangle$ and $\langle 110 \rangle$ direction are asymmetric. For a Ga-terminated surface the same is valid, but the $\langle 110 \rangle$ and $\langle 1\bar{1}0 \rangle$ directions are interchanged. Note, that this in-plane asymmetry explains the in-plane uniaxial magnetocrystalline anisotropy [17, 30].

V. MAGNETIC PROPERTIES

In Fig.5 we show the average Fe magnetic moment as a function of the Fe thickness for the Fe_i and $Fe_s + Ga_i$ IC. Surprisingly, we calculate for the thickness of 1 ML of Fe the Fe magnetic moment to be zero. In Fig.6 we

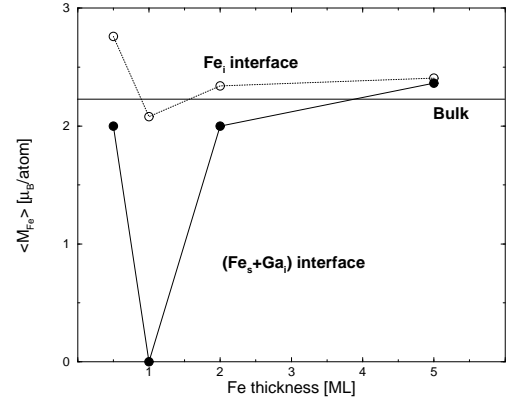


FIG. 5: Average Fe magnetization, $\langle M_{Fe} \rangle$, as a function of the Fe film thickness for two interface configurations. Solid (dotted) line corresponds to the $Fe_s + Ga_i$ (Fe_i) IC. The solid horizontal line indicates the calculated Fe bulk magnetic moment.

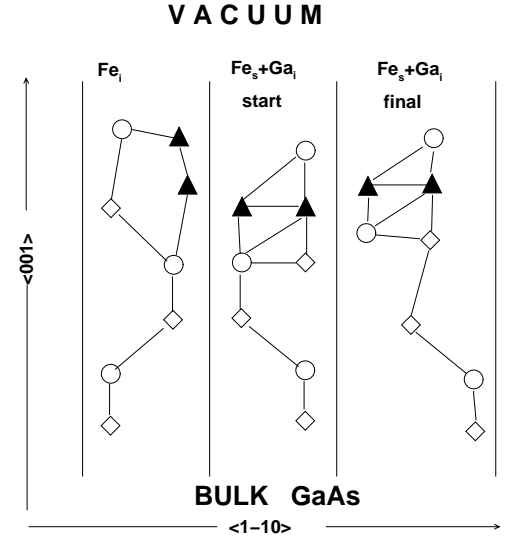


FIG. 6: Geometrical structure of 1 ML Fe on top of GaAs(100). Circles (diamonds) represent As (Ga) and triangles represent Fe. The three columns correspond to three different configurations as discussed in the text.

show the atomic

configuration for Fe_i and $Fe_s + Ga_i$ for the Fe thickness of 1 ML. It can be seen by comparing the starting and final positions, that for $Fe_s + Ga_i$ the Fe-As bond distance has decreased (tab.2). In addition the 'vertical' Ga-As bonds are broken and the three top layers became shifted along the $\langle 11\bar{0} \rangle$ direction. This suggests that the three top layers now form a separate 2-dimensional phase.

In order to understand the decreased magnetic moment, we plot in Fig.7 the Fe magnetic moment as a function of the Fe-anion distance, D , (i.e. the Fe-As distance) for all different configurations that we have calculated. It can be seen that for $D = 2.36$ Å, the magnetic moment disappears. We interpret this to be

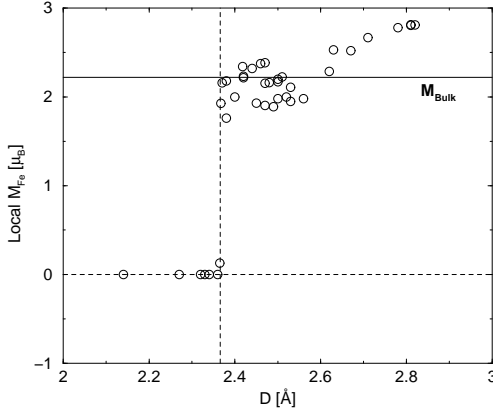


FIG. 7: Local magnetic moment of Fe, M_{Fe} , as a function of the Fe-As distance, D . Solid (dashed) horizontal line indicates the bulk Fe magnetic moment (zero-line) and the dashed vertical line at 2.37 Å indicates the Fe-As distance at which the Fe magnetic moment becomes zero.

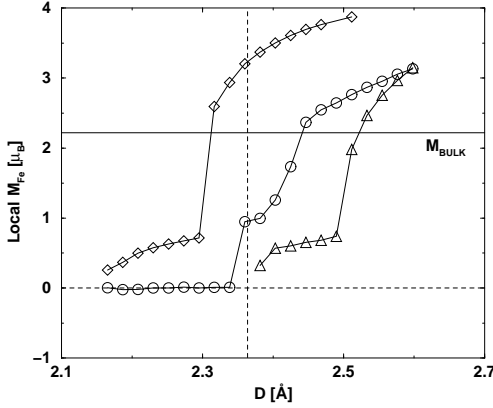


FIG. 8: Bulk magnetic moment per Fe atom for zincblende FeAs (circles), zincblende FeSe (diamonds), and zincblende FeTe (triangles) as a function of the Fe-anion distance, D . The dashed vertical line is the same as in Fig. 7 shown here for comparison.

caused by pd -hybridization: The Fe spin-polarization is driven by the on-site exchange interaction. Therefore the Fe magnetic moment decreases with increasing delocalization of the Fe d -states. Because, the delocalization of the Fe d -states increases with increased overlap between the Fe d -states and As p -states, we find that the Fe magnetic moment is quenched for small Fe-As bond distances. The spread in magnetic moments for bond lengths above 2.36 Å is due to the other factors influencing the Fe magnetic moment, like number of Fe neighbours and number of vacant neighbours.

Our interpretation is supported by the behaviour of the Fe magnetic moment in the bulk FeAs zincblend compound (circles in Fig.8). We show the Fe magnetic moment as a function of the Fe-anion distance (D) in the zincblend lattice. The same trend as before is observed, namely the Fe magnetic moment becomes smaller at a

critical D . In contrast to Fe on GaAs, the Fe magnetic moment is not quenched on ZnSe [31]. In order to understand the difference between GaAs and ZnSe we also calculated zincblende FeSe and for comparison zincblende FeTe. In all three cases, i.e. FeAs, FeSe, and FeTe, the Fe d -electrons hybridize with the respective anion's p -electrons. Therefore there exists a bond distance at which the Fe magnetic moment becomes quenched (Fig.8). The exact value of the critical D depends on the system in question. For a given lattice constant (set by for example the semiconductor host), the anion will occupy a certain fraction of the unit cell volume that depends on its atomic radius. GaAs and ZnSe have about the same lattice constant. The As atomic radius (1.14 Å) is larger than the Se radius (1.03 Å). The pd -overlap between Fe and Se is therefore (for the same lattice constant) smaller than between Fe and As and the Fe magnetic moment starts to become quenched for a smaller D . On the other hand the Te radius (1.23 Å) is larger and the magnetic moment becomes quenched already for a larger D .

As clearly visible from Fig.8 there exist high-spin, low spin, and zero moment phases as a function of D . The energy difference between these phases becomes rather small for a given D . This will be further investigated in the future. We conclude that the magnetic configuration of Fe on GaAs will be determined by pd -hybridization, but that the specific magnetic phase of the Fe-As complex depends on small variations of the Fe-As bonding. For example, in earlier publications [19, 20] an antiferromagnetic (AFM) solution of the Fe film has been discussed and calculated. Especially for the 1 ML thick Fe film an AFM solution was found. We also investigated the possibility of an AFM solution. For a 1 ML Fe film covered with a complete ML of As we find an AFM solution for a Fe_s interface configuration ($0.22\mu_B$, $-0.22\mu_B$). The involved magnetic moments are so small because of the Fe-As pd -hybridization as discussed above. The total energy is 3 meV higher than a solution with a zero magnetic moment on both Fe sites, i.e. the AFM solution is almost degenerate with the zero moment per Fe atom solution. For the $Fe_s + Ga_i$ interface configuration we again find an AFM solution ($0.05\mu_B$, $-0.05\mu_B$) being 10 meV higher than a solution having a total magnetic moment of $0.5\mu_B$. Another example we find from our calculations is a ferrimagnetic solution. The structure consists of a 5 ML thick Fe film on top of GaAs covered with 0.5 ML As and an additional 0.5 ML As within the Fe film. The top Fe atom has a magnetic moment of $-2.1\mu_B$, whereas the two Fe atoms/cell in the next layer beneath have a magnetic moment of $0.95\mu_B$ and $1.2\mu_B$, respectively. Below this layer the additional 0.5 ML As is located. The rest of the Fe atoms have a magnetic moment close to or larger than the bulk value. The average magnetic moment for this ferrimagnetic solution is $1.55\mu_B$ per Fe atom.

Since the magnetic phase diagram of the Fe-As interaction is rather complex, it very much depends on small details of the Fe film configuration which magnetic mo-

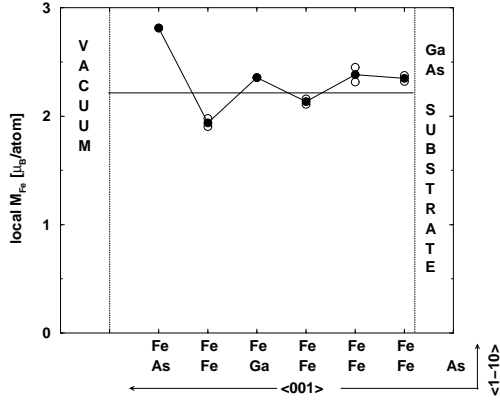


FIG. 9: Local Fe magnetic moment, M_{Fe} , profile for 6ML Fe (10 Fe atoms/cell) on top of GaAs covered with 0.5 ML As and 0.5 ML Ga within the Fe film. The horizontal line indicates the calculated bulk Fe magnetic moment. The filled (open) circles correspond to the average (individual) Fe magnetic moment of the respective layer. On the x-axis the atomic structure is sketched along the $\langle 001 \rangle$ direction projected on the $\langle 1\bar{1}0 \rangle$ direction.

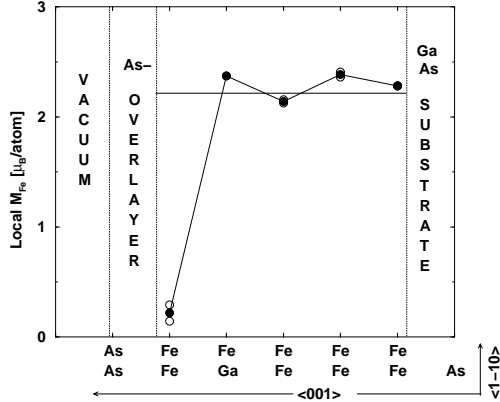


FIG. 10: Same as Fig.9, but for 5ML Fe (9 Fe atoms/cell) covered with 1ML As.

ment will be measured. But the physical mechanism behind the reduction of the Fe magnetic moment on top of GaAs is without any doubt the Fe-As *pd*-hybridization.

As can be seen from Fig.5, the Fe magnetic moment is larger for Fe_i than for $Fe_s + Ga_i$. In general the $Fe_s + Ga_i$ configuration has a smaller Fe-As bond distance than Fe_i , which explains the smaller magnetic moment for the $Fe_s + Ga_i$ configuration. For 1.5 and 2 ML of Fe , the energy gain due to increased Fe-As binding is smaller than the energy gain due to the increased spin-polarization of the Fe atoms. This explains why Fe_i is lower than $Fe_s + Ga_i$ for 1.5 and 2 ML of Fe (see discussion above and Fig.4)

In Figs.9 and 10 we show the structure and magnetic profile of a 5ML Fe film on top of GaAs(100) with one Ga atom within the Fe film for two segregation profiles: In Fig.9 for 0.5 ML As (i.e one As surface atom per cell) on top of the Fe film; in Fig.10 for 1 ML As (i.e two As

atoms per cell) on top of the Fe film. The Ga atom does not influence the Fe magnetic moment, i.e the Ga-Fe interaction is very weak. On the other hand, the Fe-As interaction quenches the magnetic moment (as discussed before). For the 1ML As coverage, the Fe magnetic moment of the top Fe layer is thus almost zero (Fig.10). If Fe is covered with only 0.5 ML As, the Fe-Fe interaction is stronger than the Fe-As interaction and the Fe magnetic moment is not reduced (Fig.9).

From our calculations we can conclude:

$$E_{Fe}^{xc} > E_{Fe-As}. \quad (3)$$

$$E_{Fe-As} > E_{Fe}^{xc} + E_{Fe-Fe}. \quad (4)$$

$$E_{Fe}^{xc} + E_{Fe-Fe} > E_{As-Fe-As}. \quad (5)$$

Here E_{Fe-As} is the Fe-As surface bond formation energy, E_{Fe}^{xc} is the energy gain due to the spin-polarization of the Fe atom, E_{Fe-Fe} is the Fe-Fe surface bond formation energy, and $E_{As-Fe-As}$ is the bond formation energy between a Fe surface atom bonded to two As atoms. These three equations explain the calculated magnetic properties.

Equation 3:

This equation states that the Fe magnetic moment will be quenched if Fe only has one or more As neighbours. For example, the Fe magnetic moment becomes zero for 0.5 ML Fe with a Fe_s IC (Fig.3). Here the Fe atom has no other Fe around it but an As atom.

Equation 4:

This equation states that the Fe magnetic moment is not quenched if the Fe atom is close to one As atom and at least one Fe atom. This is the case for the Fe_i IC of 1ML Fe on top of GaAs (Fig.6 and tab.2).

Equation 5:

The Fe magnetic moment becomes quenched again, if Fe is bonded to two As atoms (Fig.10, Fig.6), independent on the number of Fe neighbours.

For completeness, we show in Fig.11 the spin-polarization of the GaAs host. The Fe magnetic moment is not shown here (see Fig.10). The induced spin-polarization is mostly antiparallel and rather small.

In a recent X-ray absorption study [12], the number of Fe 3d-holes was determined as a function of the Fe film thickness on *n*-doped GaAs. Freeland et al find the number of holes to increase with decreasing Fe film thickness. They explain this due to charge transfer from Fe to As which they also believe to be the cause for the reduced Fe magnetic moment.

Our calculation describes the charge transfer between Fe and *p*-doped GaAs, because due to numerical reasons the Fermi energy of bulk GaAs is fixed at the top of the valence band edge. From our calculations we directly get the number of Fe 3d-holes as a function of the Fe film thickness (Fig.12). Our absolute number of the Fe

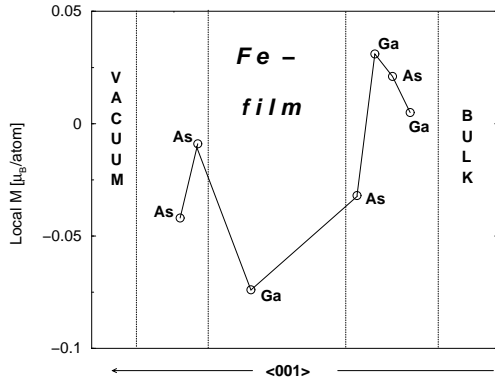


FIG. 11: Local magnetic moment, M , profile of Ga and As for the geometrical structure of 5 ML Fe on top of GaAs covered with 1 ML As and 0.5 ML Ga within the Fe film. The Fe magnetic moment is not shown here.

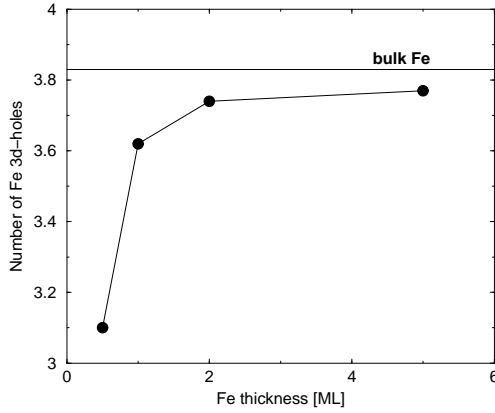


FIG. 12: Calculated number of Fe 3d-holes as a function of the Fe film thickness. The horizontal line indicates the number of Fe 3d-holes for Fe bulk.

3d-holes depends of course on the chosen Wigner-Seitz radius for Fe, but the trend we find to be independent on the chosen Wigner-Seitz radius. In contrast to experiment we find an increase of the holes with increasing Fe film thickness.

Our explanation is the following: The Fe-As pd -hybridization determines the Fe magnetic moment, not a charge transfer between Fe and As. The electron transfer between Fe and GaAs is different for n -type and p -type conditions, because for n -type (p -type) GaAs, the Fermi level of Fe has to align with the conduction (valence) band of GaAs. Under p -type conditions, a consequence of the hybridization is that on average there are slightly more delocalized electrons on the Fe site, i.e. the number of 3d-holes decreases. The thicker the Fe film becomes, the more Fe atoms are without an As neighbour, which is why the number of d -electrons (holes) decreases (increases) with increasing Fe thickness. Under n -type conditions it is plausible to assume vice versa that on average there are slightly less delocalized electrons on the Fe site. We therefore predict that the experimentally ob-

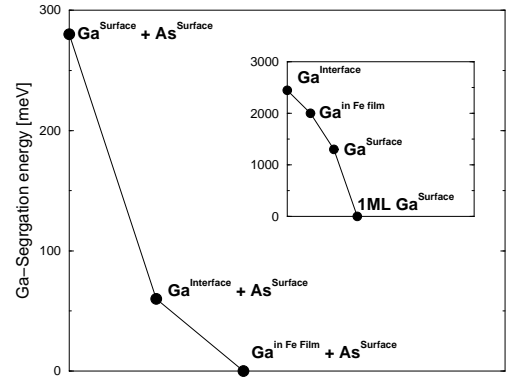


FIG. 13: Ga segregation energy for four different Ga configurations as discussed in the text for 5ML Fe on top of GaAs.

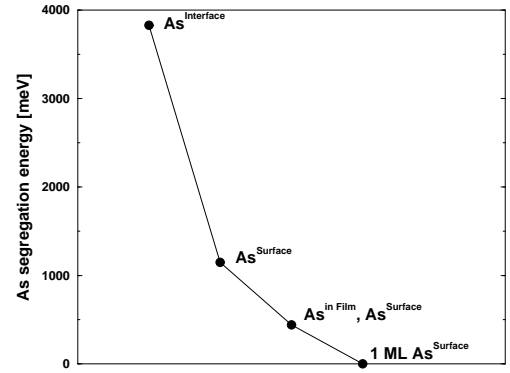


FIG. 14: As segregation energy for four different As configurations as discussed in the text for 5ML Fe on top of GaAs.

served charge transfer differs between p -doped GaAs and n -doped GaAs and that similar experiments performed instead on p -doped GaAs should find an increase of the 3d-holes with increasing thickness in agreement with our calculations.

VI. SURFACE SEGREGATION

It is well known that at metal-semiconductor interfaces the semiconductor constituents segregate towards the surface. For example, for Fe on GaAs it is known that As segregates to the surface, whereas Ga is not found at the surface but within the metal film [14, 15, 16]. It is found that the segregation of As is independent of temperature, but the segregation of Ga is dependent on temperature. A quantitative understanding of segregation is obtained with a simple model put forward by Weaver et al. [32]. The free energy of segregation is determined by the strain energy and surface energy, the latter of which they estimated with the cohesive energy. Their model predicts for Fe on GaAs both Ga and As to segregate to the surface, whereas in experiment only As surface segregation is observed. In the following we resolve this discrepancy.

In Figs.13 and 14, we show the Ga (respective As) seg-

regation energy relative to the energetically lowest configuration. For Ga we have to consider two cases separately: (i) no As has segregated to the surface and (ii) As has segregated to the surface. In case (i) (insert of Fig.13), Ga prefers to segregate to the surface (1ML $\text{Ga}^{\text{Surface}}$). The segregation energy of 1ML Ga amounts to 2.4 eV. In case (ii) where As already has segregated to the surface (Fig.13), Ga prefers to leave the interface ($\text{Ga}^{\text{Interface}}$) and stay somewhere within the Fe film ($\text{Ga}^{\text{inFe-film}}$). It is more costly (280 meV) for the Ga to be in the surface layer together with an As atom ($\text{Ga}^{\text{Surface}}$). Therefore, if As has segregated to the surface, no Ga will be found at the surface.

The As segregation energy (Fig.14) shows the same trend as the Ga segregation energy (inset of Fig.13), but the segregation energy of one As atom to the surface is 1.5 eV larger than for one Ga atom. Notice, that both Ga and As prefer to be within the Fe film rather than at the interface. In summary, this suggests the following: On top of the Fe film always As will be found independent of the GaAs surface termination. The segregation profiles should more or less be independent on the GaAs surface termination, because the Fe-As interaction is much stronger than the Fe-Ga interaction.

The As segregation path is a result of the lattice relaxation due to the chemical interaction between the Fe and As, which implies that As segregates already at $T = 0$ K. The segregation is thus **not** diffusion controlled, but only controlled by chemical bonding, which is in agreement with experiment. We find Ga to leave the interface, but only to segregate to the surface, if no As already has segregated. In contrast to As, the segregation of Ga, does not take place at $T = 0$ K. There exists an activation barrier for the segregation, i.e. the segregation is diffusion controlled. The amount of Ga on top of or within the Fe film is therefore strongly dependent on temperature, whereas the amount of As on top of the Fe film is only weakly dependent on temperature. This is in agreement with an experimental study of the Fe/GaAs interface interdiffusion [6].

Regarding the Weaver model, we find that Ga segregates to the surface (in agreement with the Weaver

model), if no As has segregated. If As has segregated, Ga will stay within the Fe-film (in agreement with experiment).

VII. DISCUSSION AND SUMMARY

We find As to segregate to the surface on top of the Fe film independent of termination, which is in agreement with experiments. The Fe/GaAs interface is not stable against further segregation. An As atom within the Fe film has a lower energy than at the interface. In an experiment one will thus always find As within the Fe film, where the Fe-As *pd*-hybridization will quench the Fe magnetic moment. Since Ga also has a lower energy within the Fe film than at the interface, one will also always find Ga within the Fe film. Ga itself does not influence the magnetic moment (Fig.9), but probably Ga in the Fe film will prevent further As segregation. This would explain the much lower thickness of the magnetically quenched Fe layers for Ga terminated samples. The thickness of the magnetically quenched Fe layers is then determined by the probability of finding As and Ga within the Fe film. This probability depends on the termination and the Fe growth conditions. Our results presented here for Fe on GaAs are most likely also valid for other semiconductor substrates. For example, we find more or less the same structures for Fe on ZnSe [31] and the segregation behaviour is the same, but the Fe-Se hybridization is much weaker.

Acknowledgments

We are grateful to the Swedish foundation for strategic research (SFS), the Swedish Research Council (VR), the Göran Gustafsson foundation, and the European RTN network on "computational spintronics" for financial support. We thank the Swedish supercomputer center (SNAC) for providing us with supercomputer time.

-
- [1] G.A.Prinz, Science **282**, 1660 (1998).
 - [2] H.J. Zhu, M. Ramsteiner, H. Kostial, M. Wasserman, H.-P. Schönherr, and K.H. Ploog, Phys. Rev. Lett. **87**, 016601 (2001).
 - [3] J.J. Krebs, B.T. Jonker, and G.A. Prinz, J. Appl. Phys. **61**, 2596 (1987).
 - [4] A. Filipe, A. Schuhl, and P. Galtier, Appl. Phys. Lett. **70**, 129 (1997).
 - [5] M. Gester, C. Daboo, R.J. Hickens, S.J. Gray, A. Ercole, and J.A.C. Bland, J. Appl. Phys. **80**, 347 (1996).
 - [6] M. Rahmoune, J.P. Eymery, and M.F. Denanot, J. Magn. Magn. Mater. **175**, 219 (1997).
 - [7] C. Lallaizon, B. Lepine, S. Ababou, A. Guivarch, S. Deputier, F. Abel, and C. Cohen, J. Appl. Phys. **86**, 5515 (1999).
 - [8] F. Bensch, G. Garreau, R. Moosbühler, E. Beaurepaire, and G. Bayreuther, J. Appl. Phys. **89**, 7133 (2001).
 - [9] Y.B. Xu, M. Tselepi, C.M. Guertler, C.A.F. Vaz, G. Wastlbauer, and J.A.C. Bland, J. Appl. Phys. **89**, 7156 (2001).
 - [10] F.P. Zhang, P.S. Xu, E.D. Lu, H.Z. Guo, F.Q. Xu, and X.Y. Zhang, J. Appl. Phys. **86**, 1621 (1999).
 - [11] R.A. Gordon, E.D. Crozier, D.-T. Jiang, T.L. Monchisky, and B. Heinrich, Phys. Rev. B **62**, 2151 (2000).
 - [12] J. W. Freeland, I. Coulthard, A.P.J. Stampfl, and W.J. Antel, Phys. Rev. B **63**, 193301 (2001).
 - [13] G. Wedler, B. Wassermann, R. Nötzel, and R. Koch, Appl. Phys. Lett. **78**, 1270 (2001).

- [14] S.A. Chambers, F. Xu, H.-W. Chen, I.M. Vitomirov, S.B. Anderson, and J.H. Weaver, Phys. Rev. B **34**, 6605 (1986).
- [15] M.W. Ruckman, J.J. Joyce, and J.H. Weaver, Phys. Rev. B **33**, 7029 (1986).
- [16] E.M. Kneedler, B.T. Jonker, P.M. Thibado, R.J. Wagner, B.V. Shanabrook, and L.J. Whitman, Phys. Rev. B **56**, 8163 (1997).
- [17] M. Brockmann, M. Zölfl, S. Miethaner, and G. Bayreuther, J. Magn. Magn. Mater. **198**, 384 (1999).
- [18] S. Hirose, S. Haneda, M. Yamaura, K. Hara, and H. Munekata, J. Vac. Sci. Technol. B **18**, 1397 (2000).
- [19] S. C. Hong, M.S. Chung, B. G. Yoon, and J.I. Lee, J. Mag. Magn. Mat. **239**, 39 (2002).
- [20] S. T. Erwin, S. H. Lee, and M. Scheffler, Phys. Rev. B **65**, 205422 (2002).
- [21] M. Kosuth, J. Minar, I. Cabria, A.Y. Perlov, V. Crisan, H. Ebert, and H. Akai, Phase Transitions **75**, 113 (2002).
- [22] G. Kresse and J. Hafner, Phys. Rev. B **47**, RC558 (1993); G. Kresse and J. Furthmüller, Phys. Rev. B **54**, 11169 (1996).
- [23] P.E. Blöchel, Phys. Rev. B **50**, 17953 (1994).
- [24] J. P. Perdew and Y. Wang, Phys. Rev. B **45**, 13244 (1992).
- [25] H. J. Monkhorst and J. D. Pack, Phys. Rev. B **13**, 5 188 (1976).
- [26] K. Shiraishi, J. Phys. Soc. Jpn. **59**, 3455 (1990).
- [27] A. Eichler, J. Hafner, J. Furtmüller, and G. Kresse, Sur. Sci. **346**, 300 (1996).
- [28] D. K. Biegelsen, R. D. Bringans, J. E. Northrup, and L.-E. Schwartz, Phys. Rev. B **41**, 5701 (1990); N. Moll, A. Kley, E. Pehlke, and M. Scheffler, Phys. Rev. B **54**, 8844 (1996).
- [29] S.-H. Lee, W. Moritz, and M. Scheffler, Phys. Rev. Lett. **85**, 3890 (2000).
- [30] E. Sjöstedt, L. Nordström, F. Gustavsson, and O. Eriksson, accepted for publication in Phys. Rev. Lett. .
- [31] B. Sanyal and S. Mirbt, Phys. Rev. B **65**, 144435 (2002).
- [32] J. H. Weaver, Z. Lin, and F. Xu in 'Surface segregation phenomena'/ editors P. A. Dowben and A. Miller, 1990.